URSI GASS 2021, Rome, Italy, 28 August - 4 September 2021

Simulation based channel hardening of cell-free massive MIMO in mm-Wave

C. Qin[1,2], Y. Gao[1], J. Chen[1], A.A. Glazunov[2,3] and J. Zhang[1,4]
(1) Ranplan Wireless Network Design Ltd., Cambridge, U.K.
(2) University of Twente, Enschede, the Netherlands
(3) Chalmers University of Technology, Gothenburg, Sweden
(4) University of Sheffield, Sheffield, U.K.

Abstract

In this paper, the spatial distribution of the channel hardening of cell-free massive MIMO array antenna topologies for mm-Wave communications is explored. The simulation of the propagation channels was performed by means of ray tracing computations. The channel hardening is evaluated in two different radio wave propagation channel conditions: first, an indoor office room furnished with desks, chairs and shelters and secondly, the same room without furniture. The spatial distribution of the channel hardening is investigated in both scenarios as a function of the number of antenna elements of the array. The simulation results show that the channel hardening effect is as expected larger in the furnished room as compared with the empty room. Also as expected, the channel hardening increases with the number of antenna elements. An interesting new observation is that the channel hardening is not uniformly distributed within the coverage area. Indeed, for the considered cell-free array antenna topologies and indoor propagation scenarios the channel hardening effect becomes lesser the closer the user gets to the antenna locations and near the walls of the rooms.

1 Introduction

Three key features of 5G networks are the massive multiple-input multiple-output (MIMO) antenna systems, the millimeter Wave (mm-Wave) frequency spectrum allocation and the ultra-dense deployment of Small Cells (SC) [1]. Massive MIMO improves the spectrum efficiency allowing several users to share the same time-frequency resource by Multiuser MIMO (MU-MIMO) techniques. Furthermore, the mm-Wave bands offer larger chunks of available frequency bandwidths, but also, due to the shorter wavelengths, it enables the use of massive MIMO array antennas with many elements mounted in a base station or access point contributing to larger spectrum efficiency. The larger bandwidth translates directly to higher capacity and data rates [2]. The dense deployment of SC improves the capacity per unit area by reusing the frequency resource in a smaller coverage area. In addition to higher spectrum efficiency, another key advantage of massive MIMO systems is higher reliability [3, 4], which is essential for applications such as remote surgery, intelligent transportation systems and industry automation.

The typical spatial deployments of massive MIMO array antenna are the co-located, the split and the cell-free (or the distributed) topologies. Cell-free massive MIMO was firstly introduced in [5] aiming at providing uniform service in large coverage areas. In a cell-free array antenna topology, the antenna elements are deployed in a distributed manner, so that all the users can be served by the antennas that have the best channel propagation conditions. In this way, the cell edge limitation can be overcome and the benefits arising from macro-diversity can be exploited.

In a massive MIMO system, as the number of the antennas increases, the variations of the channel gain decrease over the time, the frequency and the spatial domains. The channel gain becomes concentrated around its mean, i.e., the channel becomes more deterministic. This phenomenon is known as channel hardening. It has an impact on the practical design of massive MIMO systems, e.g., improved reliability due to less variations and decrease the need of downlink pilots.

The study of channel hardening has mainly focused on variations over frequency or time, due to its impact on decreasing delay spread and the coherent combination of signals from a large number of antennas, respectively [5]. In papers [3] and [4], the theory of channel hardening has been discussed. In papers [6] and [7], the authors have investigated the channel hardening phenomenon based on measurement data. In [8], the channel hardening is investigated based on simulation results in real scenarios based on ray tracing channel simulations considering different array antenna topologies deployed in different radio wave propagation conditions. Paper [9] evaluated the cell-free massive MIMO system based on realistic stochastic antenna deployment method and revealed that channel hardening only appears for low pathloss exponents (e.g. $\alpha < 2$) environments. In paper [10], the impacts of channel hardening with spatial correlation, line-of-sight (LOS) components and user-centric strategies of cell-free massive MIMO system were analyzed. As to the spatial distribution of channel hardening for cell-free massive MIMO, not as many studies have investigated this phenomenon.

The deployment of current cellular networks has been mainly restricted to sub-6GHz frequencies at the μwave bands. Although these frequency bands show favorable propagation conditions, they cannot measure up with the key features of mm-Wave 5G networks. As a matter of fact, the channel propagation characteristics at mm-Wave and at μwave are rather different. For example, propagation at mm-Wave is mainly based on the LOS due to the higher penetration and diffraction losses. Paper [2] investigated six key differences between massive MIMO at μwave and massive MIMO at mm-Wave. Many other papers have studied the combination of massive MIMO with mm-Wave frequency bands (see, e.g., [11, 12]). However, to the best knowledge of the authors, no publication has focused on the spatial channel hardening effects of cell-free massive MIMO at the mm-Wave frequencies.

In this paper, we extend our analysis in [8] by considering the channel hardening at mm-Wave as well as the spatial distribution of channel hardening. The simulation analyses are based on a cell-free massive MIMO array antennas topology deployed in two different radio wave propagation conditions. Heat maps and the corresponding cumulative distribution functions (CDF) of the spatial distribution of the channel hardening effect are given based on numerical simulations. The study considers cell-free massive MIMO array antenna with various numbers of antenna elements deployed in the two different propagation scenarios. The results show the channel hardening effect is quite different at the different locations of the room for both the furnished room and the empty room. This is because the high propagation loss at the mm-Wave frequency band, which also highly differs in the non-line-of-sight (N-LOS) and the LOS conditions.

2 Channel Hardening

Let's assume a massive MIMO system comprising an array antenna with M antenna elements and K single antenna users. The channel between the M antenna elements and the k-th user is an M×1 complex channel vector, defined by

$$\mathrm{g_k(t)} = \left[\sqrt{\beta_{\mathrm{k,1}}}\mathrm{h_{k,1}} \quad \sqrt{\beta_{\mathrm{k,2}}}\mathrm{h_{k,2}} \quad \dots \quad \sqrt{\beta_{\mathrm{k,M}}}\mathrm{h_{k,M}}\right]^{\mathrm{T}}, \tag{1}$$

where, $\beta_{\mathrm{k,m}}$ and $\mathrm{h_{k,m}}$ are the large scale fading and time-variant small scale fading channel coefficients, respectively. $[\cdot]^{\mathrm{T}}$ denotes the matrix transpose operation. While $\beta_{\mathrm{k,m}}$ is constant over multiple coherence intervals, $\mathrm{h_{k,m}(t)}$ is time varying.
The channel hardening is defined as

$$\frac{\mathrm{var}\{\|\mathrm{g}_k(\mathrm{t})\|^2\}}{\mathrm{E}\{\|\mathrm{g}_k(\mathrm{t})\|^2\}^2} \to 0, M \to \infty, \tag{2}$$

where $\|\mathrm{g}_k(\mathrm{t})\|$ is the Euclidean Norm of the channel vector at the t time slot. var $\{\cdot\}$ and E $\{\cdot\}$ denote the variance and the mean, respectively. The statistics are computed over the time realizations.

The norm of equation (1) is computed as

$$\|\mathrm{g}_k(\mathrm{t})\|^2 = \sqrt{\sum_{\mathrm{m=1}}^{\mathrm{M}} \beta_{k,m}\left|\mathrm{h_{k,m}(t)}\right|^2}, \tag{3}$$

which represents the total power received by the k-th user.

3 Simulation Scenarios

The radio propagation channel is simulated by means of the Ranplan Professional software [13], which is a 3D ray tracing tool. It considers the 3D building structures, the material electric properties, as well as the radiation pattern of the antenna [8]. It has the capability to capture the complex channel gain considering large-scale fading and small-scale fading of a real 3D scenario. It supports propagation channel simulation up to 70 GHz frequency bands, which has been tested and validated in the literature [14]. The output of this propagation engine includes the complex path gain and the power delay profiles (PDP), from which the channel transfer function can be calculated based on the channel model specification defined by 3GPP [15].

The simulation results are used to estimate the spatial distribution of the channel hardening effect at different locations in two scenarios. One is an office room furnished with desks, chairs, and shelters, the other is an empty room with the same size and walls layout as the furnished room (see Figure 1). The cell free massive MIMO array antenna topology with different numbers of antennas are simulated. The parameters of the simulation scenarios are listed in Table 1.

Table 1. Simulation scenario parameters

Simulator tool	Ranplan Professional
Propagation model	3D ray tracing
Size of scenarios	50×120×3 m^3
Height of desks	90 cm
Height of chairs	90 cm
Height of shelters	1.5 m
Height of Tx antennas	2.4 m
Frequency	26 GHz
Number of Tx antennas (M)	4, 16, 32, 64
Array antenna topologies	Cell-free
Antenna type	Isotropic
Minimum antenna distance	5.1m
Maximum antenna distance	50.0 m
Height of users	1.0 m
Simulation resolution	0.5 m
Number of snapshots	10,000

Cell-free massive MIMO array antenna topologies with 4, 16, 32 and 64 antennas are considered. All the antennas are distributed according to a uniform distribution along the perimeter comprised by the outer wall of the room, which is the same for the two scenarios. Figure 1. (a) and (b) show

a 3D view of 64 cell-free massive MIMO antenna system deployed in the furnished and the empty rooms, respectively.

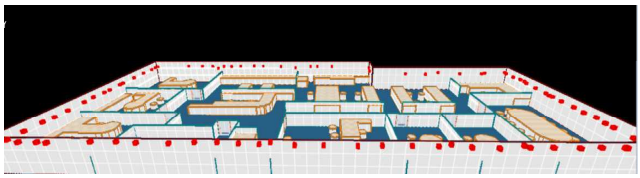

(a) 64 cell-free antennas deployed in the furnished room

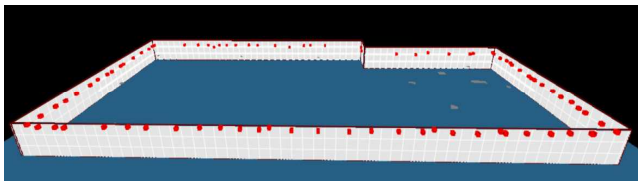

(b) 64 cell-free antennas deployed in the empty room

Figure 1. 3D view of the scenarios and antennas

4 Numerical Results

2D heat maps representing the spatial distribution of the channel hardening effect in the two defined scenarios with 16 and 64 antennas are shown in Figure 2. As can be seen from the heat map, increasing the number of antennas, the channel hardening effects are enhanced in both the furnished and the empty room as expected. For both scenarios, the channel hardening effect in the areas closer to walls is much poorer than that in the middle area. The areas with poor channel hardening in the empty are evenly room distributed. On the other hand, in the furnished room the channel hardening is more inhomogeneous having areas with lesser channel hardening also in the interior of the room. This can be explained by the fact that the signals from the nearest antennas have a relatively higher signal strength than the signals from the other antennas. This results in a power imbalance that is inhomogeneous throughout the considered furnished room. Hence, only a limited number of antennas dominate in the cell-free massive MIMO system, in this way reducing the channel hardening effects at some user positions.

Figure 3 shows the cumulative distribution functions (CDFs) of channel hardening effect for the cell-free array antenna topology. As can be seen from Figure 3, in an empty room, the channel hardening effect is relatively smaller than that in the room with furniture with the same number of antennas. Take the case with 64 antennas as an example. Then, in the furnished room, 90% of the area can get the channel hardening effect (normalized variance in (3)) better than -10 dB. But in the empty room, only 65% of the area can achieve the same value. When reducing the number of the antennas to 32, less than 50% of the area can get the channel hardening effects better than -10 dB both in the furnished room and in the empty room. Increasing the number of antennas enhanced the channel hardening effect in both the empty and the furnished rooms as expected.

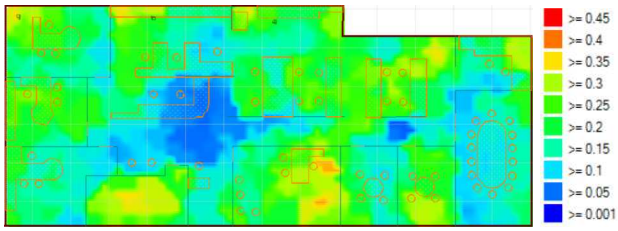

(a)

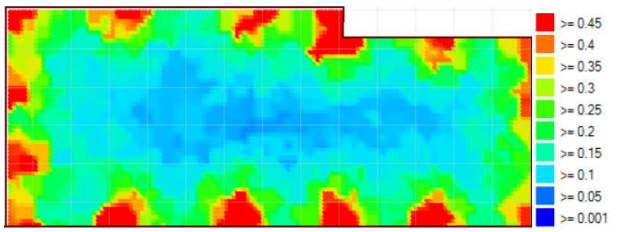

(b)

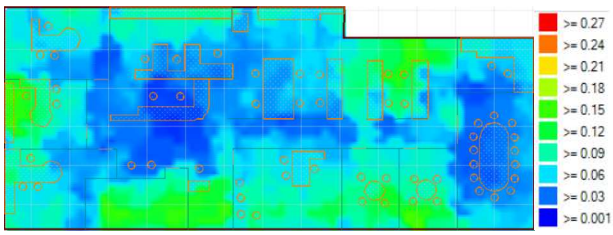

(c)

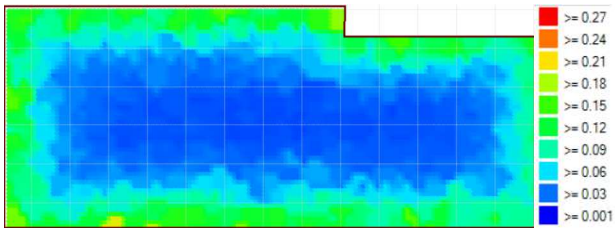

(d)

Figure 2. Spatial distribution hardening effect (a) 16 cell-free antennas deployed in the furnished room, (b) 16 cell-free antennas deployed in the empty room, (c) 64 cell-free antennas deployed in the furnished room, (d) 64 cell-free antennas deployed in the empty room.

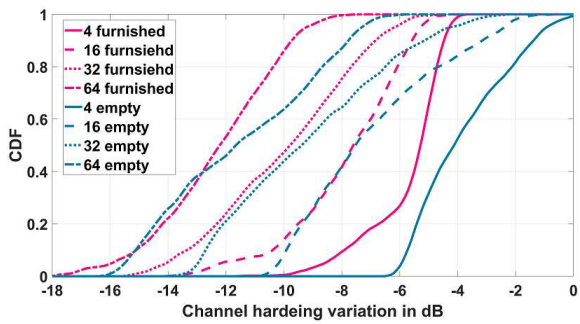

Figure 3. CDF of channel hardening variation in dB for cell- free antenna in 2 different scenarios.

The major findings of this paper are summarized as follows:

1) Channel hardening can be expected for cell-free massive MIMO in the mm-Wave frequency bands.
2) Increasing the number of massive MIMO antenna elements increases the channel hardening effects as expected.
3) The channel hardening effect in a furnished room is larger than in the same, but empty, room.
4) For the cell-free array antenna topology the areas near the antennas will have a smaller channel hardening effect.

Future work will consider other type of indoor environments as well as a comparison with various co-located and split antenna topologies.

5 Conclusions

This paper presents a simulation-based evaluation of the spatial distribution of the channel hardening in mm-Wave frequency band. A cell-free array antenna topology was evaluated in an office room with and without furniture. The comparison shows that the furnished room have a larger channel hardening effect. Channel hardening heat maps show a deeper sight of channel hardening effect in different areas of the room. This result demonstrates that the channel hardening effect in mm-Wave frequency band strongly depends on the indoor propagation environment and the user location.

6 Acknowledgements

The authors would like to acknowledge the support of the WaveComBE project, under Horizon 2020 research and innovation program with grant agreement No. 766231.

7 References

[1] T. E. Bogale and L. B. Le, "Massive MIMO and mmWave for 5G Wireless HetNet: Potential Benefits and Challenges," in IEEE Vehicular Technology Magazine, vol. 11, no. 1, pp. 64-75, March 2016, doi: 10.1109/MVT.2015.2496240.

[2] Stefano Buzzi, Carmen D'Andrea. Massive MIMO 5G Cellular Networks: mm-Wave vs. μ-Wave Frequencies[J]. ZTE Communications, 2017, 15(S1): 41-49.

[3] T. L. Marzetta, "Noncooperative cellular wireless with unlimited numbers of base station antennas," IEEE Trans. Wireless Commun., vol. 9, pp. 3590–3600, Nov 2010.

[4] E. G. Larsson, O. Edfors, F. Tufvesson, and T. L. Marzetta, "Massive MIMO for next generation wireless systems," IEEE Communications Magazine, vol. 52, no. 2, pp. 186–195, Feb 2014.

[5] H. Q. Ngo, A. Ashikhmin, H. Yang, E. G. Larsson, and T. L. Marzetta, ''Cell-free massive MIMO versus small cells,'' IEEE Trans. Wireless Commun., vol. 16, no. 3, pp. 1834–1850, Mar. 2017.

[6] S. Gunnarsson, J. Flordelis, L. Van Der Perre and F. Tufvesson, "Channel Hardening in Massive MIMO: Model Parameters and Experimental Assessment," in IEEE Open Journal of the Communications Society, vol. 1, pp. 501-512, 2020, doi: 0.1109/OJCOMS.2020.2987704.

[7] l. O. Martínez, E. De Carvalho, J. O. Nielsen, "Massive MIMO properties based on measured channels: Channel hardening user decor-relation and channel sparsity", Signals Systems and Computers 2016 50th Asilomar Conference on, pp. 1804-1808, 2016.

[8] C. Qin, Y. Miao, Y. Gao, J. Chen, J. Zhang and A. A. Glazunov, "Simulation-based Investigation on Spatial Channel Hardening of Massive MIMO in Different Indoor Scenarios and with Different Array Topologies," 2020 XXXIIIrd General Assembly and Scientific Symposium of the International Union of Radio Science, Rome, Italy, 2020, pp. 1-4, doi: 10.23919/URSIGASS49373.2020.9232421.

[9] Z. Chen and E. Björnson, "Channel Hardening and Favorable Propagation in Cell-Free Massive MIMO With Stochastic Geometry," in IEEE Transactions on Communications, vol. 66, no. 11, pp. 5205-5219, Nov. 2018, doi: 10.1109/TCOMM.2018.2846272.

[10] A. Á. Polegre, F. Riera-Palou, G. Femenias and A. G. Armada, "Channel Hardening in Cell-Free and User-Centric Massive MIMO Networks With Spatially Correlated Ricean Fading," in IEEE Access, vol. 8, pp. 139827-139845, 2020, doi: 10.1109/ACCESS.2020.3012736.

[11] L. Swindlehurst, E. Ayanoglu, P. Heydari and F. Capolino, "Millimeter-wave massive MIMO: the next wireless revolution?," in IEEE Communications Magazine, vol. 52, no. 9, pp. 56-62, Sep. 2014.

[12] S. Buzzi and C. D'Andrea, "Doubly massive mmWave MIMO systems: Using very large antenna arrays at both transmitter and receiver", 2016 IEEE Global Telecommunications Conference (GLOBECOM 2016), Washington DC, USA, 5-7 Dec. 2016.

[13] https://ranplanwireless.com/products/ranplan-professional/

[14] W. Yang, J. Huang, J. Zhang, S. Salous and J. Zhang, "Indoor Measurement Based Verification of Ray Launching Algorithm at the Ka-Band," 2020 XXXIIIrd General Assembly and Scientific Symposium of the International Union of Radio Science, Rome, Italy, 2020, pp. 1-4, doi: 10.23919/URSIGASS49373.2020.9232150.

[15] 3GPP TR 38.901 V16.0.0, Technical Specification Group Radio Access Network; Study on channel model for frequencies from 0.5 to 100 GHz (Release 16), 2019-10.